ACS OMEGA

Open Access

http://pubs.acs.org/journal/acsodf

Article

Synthesis of Plant-Mediated Iron Oxide Nanoparticles and Optimization of Chemically Modified Activated Carbon Adsorbents for Removal of As, Pb, and Cd Ions from Wastewater

Published as part of ACS Omega virtual special issue "Phytochemistry".

Ali Rehman, Abdul Naeem, Ijaz Ahmad,* Fozia Fozia, Mikhlid H. Almutairi, Madeeha Aslam, Muhammad Israr, Bader O. Almutairi, and Zia Ullah

Cite This: *ACS Omega* 2024, 9, 317−329

Read Online

ACCESS | Metrics & More | Article Recommendations

ABSTRACT: This research study was designed with the aim to prepare plant extract-mediated iron oxide nanoparticles (IONPs) and different chemically modified carbon adsorbents from the *Parthenium hysterophorus* plant and then optimize the carbon adsorbents by evaluating their adsorption applications in wastewater for the selected metal ions like arsenic (As^{3+}), lead (Pb^{2+}), and cadmium (Cd^{2+}). The Fourier transform infrared spectroscopy (FTIR) technique was used to highlight functional groups in plant-mediated IONPs and chemically modified carbon adsorbents. A scanning electron microscopy study was conducted to explain the surface morphology of the adsorbents. Energy-dispersive X-rays was used for elemental analysis and X-ray diffraction for particle size and crystallinity of the adsorbents. From the study, it was found that the best optimum conditions were pH = 5−6, initial concentration of adsorbate of 10 mg/L, dose of adsorbent of 0.01 g, contact time of 90−120 min of adsorbent and adsorbate, and temperature of 25 °C. At optimum conditions, the adsorption capacities of IONPs for arsenic (As) 144.7 mg/g, lead (Pb) 128.01 mg/g, and cadmium (Cd) ions 122.1 mg/g were recorded. The activated carbon at optimum conditions showed adsorption capacities of 46.35 mg/g for As, 121.95 mg/g for Pb, and 113.25 mg/g for Cd ion. At equilibrium, Langmuir, Freundlich Temkin, and Dubinin−Radushkevich isotherms were applied on the experimental adsorption data having the best R^2 values (0.973−0.999) by the Langmuir isotherm. High-correlation coefficient R^2 values (0.996−0.999) were obtained from the pseudo-second-order for all cases, showing that the adsorption process proceeds through pseudo second-order kinetics. The apparent adsorption energy E value was in the range of 0.24−2.36 kJ/mol. The adsorption capacity of regenerated IONPs for As gradually decreased from 144.8 to 45.67 mg/g, for lead 128.15 to 41.65 mg/g, and cadmium from 122.10 to 31.20 mg/g in 5 consecutive cycles. The study showed that the synthesized IONPs and acid-activated carbon adsorbent were successfully used to remove selected metal ions from wastewater.

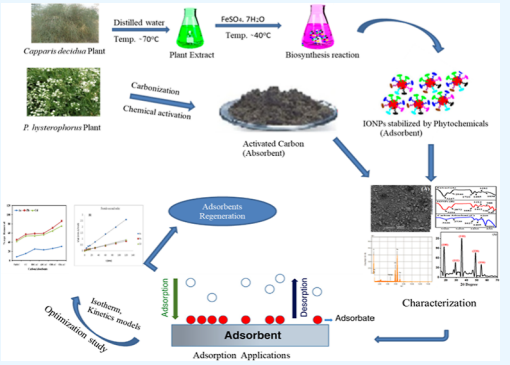

1. INTRODUCTION

Improvement in nanotechnology for drinking and wastewater handling is a matter of great concern for decision makers and researchers worldwide.[1] Although, the iron oxides have various applications in the field of environment and energy, the applications of IONP in wastewater for exclusion of heavy metal (HM) ions and other pollutants is a comparatively modern field of research. The prominent applications of IONPs in wastewater is due to its lesser toxicity, faster adsorption rate, and high adsorption affinity toward metal ions.[2] The IONPs are synthesized with various methods, such as physical, chemical,[3] and thermal decomposition,[4] hydrothermal synthesis,[5] coprecipitation,[6] sol−gel,[7] colloidal chemistry,[8] and green synthesis methods.[9] In comparison to other methods, the green synthesis method of nanoparticles is efficient and cost-effective for large-scale preparations. Contamination of water is a global concern with development of human life. Several HMs like As, Pb, and Cd that originate from anthropogenic and industrial sources are found in wastewater.[10]

HMs are toxic and among these As, Pb, and Cd are carcinogenic and cause severe health problems, like damage to the liver and brain, dysfunction of kidneys, respiratory system,

Received: July 21, 2023
Revised: November 15, 2023
Accepted: November 16, 2023
Published: December 26, 2023

and central nervous system so these HMs should be checked and removed before going inside the body.[11,12] Conventional water sources like groundwater and surface water are not capable of fulfilling the break between the demand and supply of fresh water. The rising breach may only be packed by nonrenewable and nonconventional sources like wastewater treatment. These problems offer a gap to the analysts and researchers to expose innovative resources and methods that may be operated for remarkable exclusion of metals from wastewater. Numerous wastewater treating technologies, like capacitive deionization,[13] reverse osmosis,[14] thermal distillation,[15] ion exchange,[16] and adsorption,[17,18] are exercised to get rid of the metal ions from wastewater. Among these methods, adsorption is a promising technique to treat wastewater because it is the most effective, efficient, sludge-free, regeneration efficient, and economically attractive decontamination process of wastewater, while other conventional methods have certain disadvantages like production cost, toxic sludge production, high equipment cost, high energy consumption, and non eco-friendliness.[19]

Adsorption via modified carbon and agricultural resources is owed to their effortless availability, elevated surface area, and versatile nature. Acid−base-modified activated carbon adsorbents are prepared from different types of materials. Raw material availability, adsorption properties, and cost are also important criteria for preparing an adsorbent.[20] Different adsorbents like biomaterial, seed, wood pulp, resins, chitosan, and carbon adsorbents had been tested for elimination of metal ions from wastewater[21−23] but their nonavailability, high cost, little effectiveness, hard separation, and less stability restrict their applications. The selection of plant *Parthenium hysterophorous* for unmodified and acid−base-modified activated carbon adsorbents was owed to its abundant occurrence, passive trait, invasive allelopathic effect,[24] and nonexploitation for the selected adsorbate.

The objectives of the current research were to synthesize *Capparis decidua*-mediated IONPs and optimized carbon adsorbent prepared from the *Parthenium hysterophorus* plant to adsorb the selected metal ions from wastewater. The significant novelty of this research work is to prepare various adsorbents using such modified precursors and their effectiveness for the selected metal ions, which are not reported in the literature. We hope that the current study will not only decrease the disposal problem of *P. hysterophorus* plant but it will also contribute to a low cost adsorbent for removal of selected metal ions. The research focus was on the adsorbent's adsorption capacity, optimization of different adsorption parameters, and the mechanism of adsorption and reusability of adsorbents.

2. MATERIALS AND METHODS

2.1. Synthesis of IONPs. Plant-mediated IONPs were synthesized in accordance with the procedure as outlined in the literature.[25] The selected plant *C. decidua* sample in distilled water was warmed at 40 °C for the mining of bioactive molecules. The plant-derived extract was mixed with salt and iron sulfate hepta-hydrate ($Fe_2So_4{\cdot}7H_2O$)(Purity 99%, Company: Merck) in different proportions. The solution was warmed and shook until the reddish brown color change was noted.[26] The syntheses of IONPs were confirmed by ultraviolet−visible (UV−vis)' spectroscopy. The IONPs on a large scale were prepared after the optimum ratio 3:5 of plant extract and salt. The final product was separated by centrifuge, washed out with distilled water, and calcined at 50 °C. The product was processed for further applications like characterization and adsorption studies.

2.2. Preparation of Chemically Modified Carbon Adsorbents. The selected plant *P. hysterophorus* was collected from district Karak, Khyber Pakhtunkhwa (KPK), Pakistan. Plant materials were washed with distilled water, sun desiccated, and kept in an oven for 24 h at 90 °C to get rid of further moister and was pulverized. Six different types of adsorbents were synthesized adopting various routes as reported in the literature with minor modifications.[27] Minor modifications were made with respect to the plants, adsorbates, chemicals, and temperature changes. In the first type, the selected plant *P. hysterophorous* was ground to a powder and sieved to the size <90 μm for use as an adsorbent without further modification and was labeled UnM-C. In the second type, (only carbonized) a certain amount of the selected plant powder was carbonized to obtain the carbonized sample and denoted as carbonized carbon (CC) and preserved for further studies. In the third type, (basification before carbonization), a definite quantity of chosen plant powder was mixed with potassium hydroxide (Purity 85%, company: Merck) then it was carbonized and was designated as BBC-AC. In the fourth type (acidification before carbonization), the plant powders were treated with a specific amount of phosphoric acid (H_3PO_4, Purity 99%, Company: Merck) and then carbonized for use as an adsorbent and denoted as ABC-AC. In the fifth type, (carbonization before basification) the CC was treated with potassium hydroxide in a specific ratio and was designated as CBB-AC. In the sixth type, (carbonization before acidification), the CC was treated with phosphoric acid H_3PO_4 in a specific ratio and labeled CBA-AC.

2.3. Characterization of IONPs and Carbon Adsorbent. The synthesized IONPs and carbon adsorbents were pictured out by different techniques like UV−vis, Fourier transform infrared spectroscopy (FT-IR), scanning electron microscopy (SEM), energy-dispersive X-ray (EDX), and XRD for the determination of optical properties, functional groups, surface morphologies, particle sizes, elemental analyses, and crystallinity of the adsorbents, respectively.

2.4. Adsorption Study for Optimization of Carbon Adsorbents. The batch adsorption study was conducted to determine the optimum carbon adsorbent for the exclusion of selected metal ions by using all of the prepared adsorbents. HMs like arsenic, lead, and cadmium solutions (each 1000 mg/L) were set by dissolving predefined amounts of sodium arsenate ($NaAsO_2{\cdot}12H_2O$, Purity 90%, company: Merck), lead nitrate (Pb $(NO_3)_2$, Purity 99.9%, company: Merck), and cadmium nitrate tetra hydrated ($Cd(NO_3)_2{\cdot}4H_2O$, Purity 99.99%, company: Merck) in distilled water. From this, solutions of required concentrations were made in the study. Each prepared adsorbent was subjected to the batch adsorption study for the exclusion of As, Pb, and Cd at different pH levels 2, 3, 4, 5, 6, 7, and 8 by keeping other conditions fixed like an adsorbent dose of 0.02 g, temperature of 25 °C (room temperature), and initial metal concentration of 60 ppm in 250 mL of water. The solutions were shaken by an agitator at 150 rpm for 3 h to establish an equilibrium. The contents were centrifuged at 400 rpm for 15 min. The solutions were decanted, filtered into bottles, and analyzed via a flame atomic absorption spectrophotometer (Parkin Elmer 400). These adsorption experiments were performed randomly with respect to the above parameters. All experiments were

https://doi.org/10.1021/acsomega.3c05299
ACS Omega 2024, 9, 317−329

carried out in duplicate. The percentage removal (% R) and adsorption capacities (q_e) of all the prepared adsorbents were calculated by using following I and II, respectively.

$$\% R = [(C_o - C_e)/C_o \times 100 \quad \text{(I)}$$

$$q_e = [(C_o - C_e) \times V]/M \quad \text{(II)}$$

where, C_o—adsorbate initial concentration (mg/L); C_e—adsorbate equilibrium concentration; M—mass of adsorbent (g); and V—volume of solution (L).

3. RESULTS AND DISCUSSION

The IONPs were prepared by green synthesis methods. The phytochemical constituents found in the plant extract played a fundamental role in the reduction and stabilization of the particles. The additions of iron sulfate heptahydrate solution to the plant extract turned the color of mixture reddish brown was a preliminary piece of evidence for the formation of IONPs. Analogous results were noted in the literature for synthesis of IONPs.[28] Similarly, different prepared carbon adsorbents were subjected to a batch adsorption study to get one effective and optimized carbon adsorbent after calculating the percentage adsorption and adsorption capacity of each adsorbent, the adsorbent treated with H_3PO_4 after carbonization (CBA-AC) having maximum adsorption capacity (Figure 1) against the selected metals was subjected to further studies.

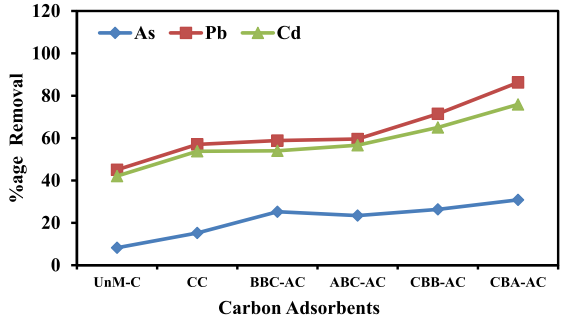

Figure 1. Optimization of carbon adsorbents.

3.1. UV−Vis Spectroscopy. The formation of IONPs was identified by monitoring the reaction mixture by using UV−vis spectroscopy. Analysis of both plant extract and IONPs was carried out in the range of 200−700 nm to get UV−vis spectra, as revealed in Figure 2. The extract spectrum shows that there was no sharp peak of the absorbance in the plant extract. The absorbance peak for IONPs was observed at 278 nm, which is in best agreement with the previous reported literature studies using IONPs synthesized from the fruit extract of *Cynometra ramiflora*.[29] The band gap energy (E) of nanoparticles was calculated by the given equation

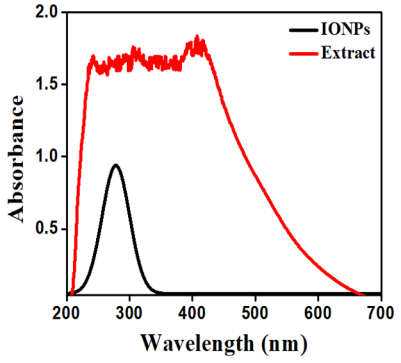

Figure 2. UV−vis spectrum of synthesized IONPs and plant extract.

$$E = hc/\lambda \quad \text{(III)}$$

where, h, c, and λ represent Planck's constant, velocity of light, and wavelength (278 nm), respectively. The (E) for the IONPs was calculated to be 4.46 eV.

3.2. FT-IR Analysis. FT-IR spectroscopy (PerkinElmer FT-IR model 1650) was performed to mark out various active groups present in the plant extract, IONPs, and carbon adsorbents. The FT-IR spectra of plant extract, IONPs, and optimized modified carbon adsorbent are shown in Figure 3A−C, respectively. The plant extract with a main peak at about 3247 cm^{-1} with a shift to 3194 cm^{-1} shows a O−H group of alcohol.[30] The peaks at 2946 to 2872 cm^{-1} was assigned to a group of CH_2 in aliphatic hydrocarbons.[31] An absorption band in the regions of 1710 and 1682 cm^{-1} indicates functional group C═O of carboxylic acid.[32] The peaks at 1485 and 1412 cm^{-1} are due to C−C stretching from the conjugated pi system of the aromatic benzene ring. Stretching vibration of N−H was confirmed by peaks around 1282 and 1212 cm^{-1} showing amide linkage that has a vital role in the reduction and stabilization of IONPs.[33] The stretching vibration of the C−N group in aliphatic amine was recorded at bands 1038 and 988 cm^{-1}. The peaks around 730 and 546 cm^{-1} show vibration of Fe−O bonds demonstrating the presence of IONPs.[25] Similarly, the FT-IR investigations of the carbon adsorbent were conducted in the range of wavenumber 400−4000 cm^{-1}. Different absorbance peaks were recorded like 3126 cm^{-1} for O−H, 2739 cm^{-1} for C−H stretching of alkenes, and 1627 cm^{-1} N−H stretching for the amine group. The shift at 1405 cm^{-1} is responsible for O−H of carboxylic acid and 1210 cm^{-1} corresponds to C−O bonds in esters. The FT-IR analyses were in reliable with the results published in the literature.[34]

3.3. SEM Analysis. IONPs were subjected to SEM for explanation of surface morphology, as revealed in Figure 4A showing that the particle size was in the range of 10−90 nm and were mostly irregular in shape. Similarly, Figure 4B shows the SEM analysis of modified carbon adsorbents of *P. hysterophorus*. The results showed that the modified carbon adsorbents has irregular surfaces and disintegrated surface morphologies. The use of carbon adsorbents modified with H_3PO_4 may have resulted in the improvement of adsorbent surface during activation. This activation is anticipated to enhance the selected metal ion adsorption.

3.4. XRD Analysis. X-ray diffraction (XRD) patterns of the prepared adsorbents was used to calculate the crystal size of the adsorbents via Shimadzu-7000 power X-ray diffractometer with 2θ range of 10−70° at room temperature. The characteristic peaks of XRD were observed at 2θ values of 18.37, 29.51, 35.24, 48.61, and 54.15°. The XRD peaks at 2θ = 18.37° (100), 29.51° (111), 35.24° (110), 48.61° (220), and 54.15° (116) of the IONPs confirm the crystalline nature. The planes at (100), (110), and (220) match the face-centered cubic nature of IONPs. The high intensity peak is in agreement with the minute nanoparticle size. The crystal size was determined by Scherrer's equation

$$\text{crystal size} = K\lambda/\beta \cos\theta \quad \text{(IV)}$$

https://doi.org/10.1021/acsomega.3c05299
ACS Omega 2024, 9, 317−329

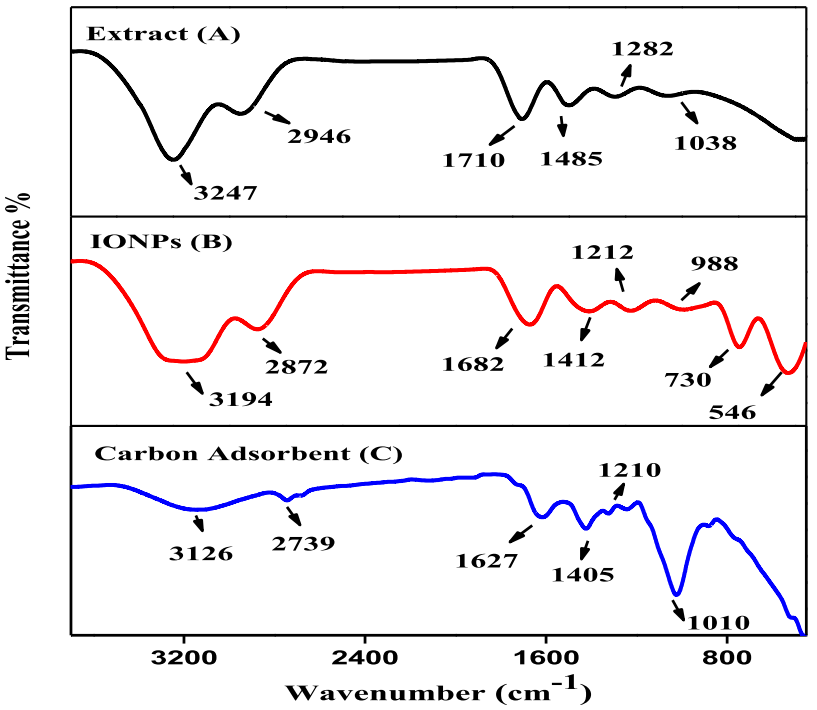

Figure 3. FT-IR spectra of (A) plant extract, (B) IONPs, and (C) carbon adsorbent.

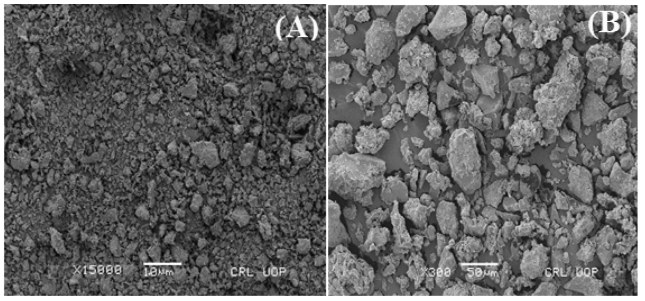

Figure 4. (A) SEM image of synthesized IONPs and (B) SEM image of modified carbon adsorbent.

In the above equation, "K" depicts shape factor (0.94), "λ" means radiations wavelength (0.154252 nm), "β" represents full width half-maximum, and Bragg's angle (radian) is denoted by θ. Similarly, the XRD pattern of the prepared carbon adsorbent was found to display the diffraction peak (111), as shown in Figure 5.

3.5. EDX Study. The synthesized adsorbents were analyzed by EDX for their elemental composition. The presences of IONPs are revealed by the high peaks of iron (Fe) and oxygen (O) in the EDX spectrum, as shown in Figure 6A,B. A high amount of Fe element was recorded in the line associated with the binding energies of IONPs with peaks around 0.7 and 6.4 keV. Some other elements like carbon and manganese were also found. Whereas, the EDX analysis of the carbon adsorbent revealed that carbon (67.92%) and oxygen (23.54%) had the highest atomic percentage. The supplementary elements in the adsorbent structure by the atomic percentage were Al (0.33%), Si (0.62%), P (6.94%), S (0.14%), Ca (0.36%), and Fe (0.15%). The presence of high contents of carbon is prime criteria for a good adsorbent.

3.6. Optimization of Adsorption Parameter Study. The IONPs and optimized carbon adsorbent were subjected to further study for optimization of several parameters effect like

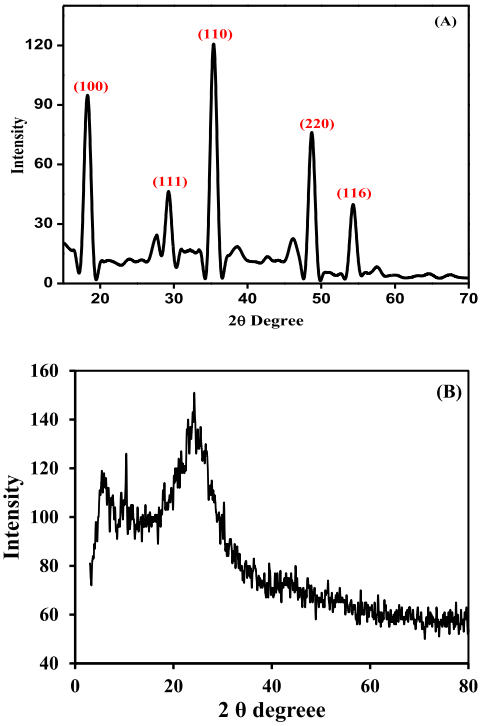

Figure 5. (A) XRD pattern of IONPs. (B) XRD pattern of modified carbon.

pH, adsorbent dose, starting adsorbate concentration, time, and temperature. During this study, one parameter was gradually changed, while other parameters were kept constant. Adsorption of arsenic, lead, and cadmium adhere to the walls of a flask was calculated by running the blank experiment and was found to be insignificant.

3.6.1. Point of Zero Charge (pH_{pzc}). A specific amount of prepared adsorbent was added to different flasks containing 50

https://doi.org/10.1021/acsomega.3c05299
ACS Omega 2024, 9, 317−329

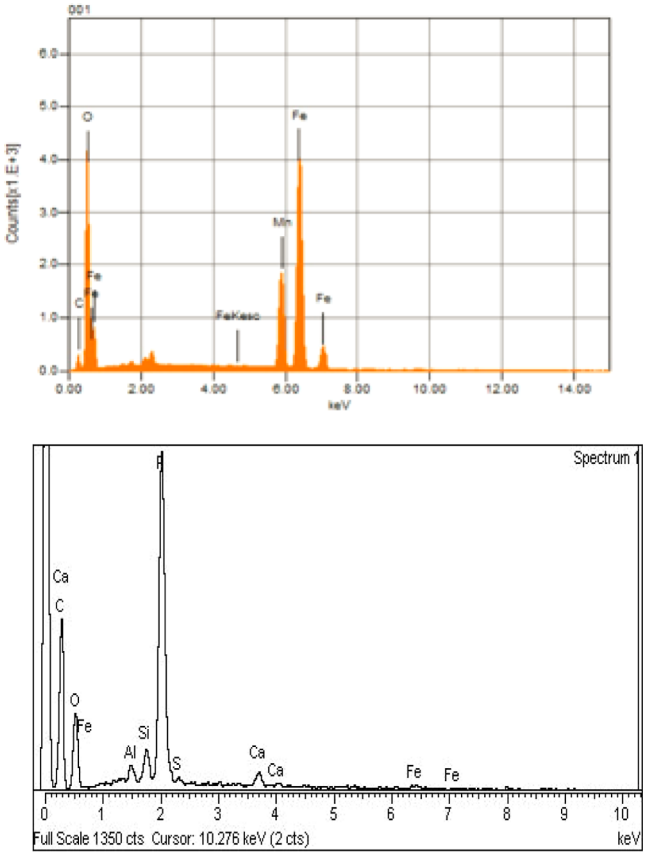

Figure 6. (A): EDX spectra of IONPs and (B): EDX spectrum of carbon adsorbent.

mL of water each with an initial pH range from 2 to 8. Nitric acid (HNO_3) 0.1 M and sodium hydroxide (NaOH) 0.1 M solutions were used to adjust the pH of the mixtures. The mixtures were shaken by an agitator at a rate of 150 rpm at 25 °C for 24 h. The equilibrium pH was determined for each solution. The change in pH (ΔpH) was calculated by means of equation given below,

$$\Delta pH = pH_{(i)} - pH_{(f)} \quad (V)$$

In the above equation, $pH_{(i)}$ is the pH of water before adding the adsorbent and $pH_{(f)}$ represents the pH after adding the adsorbent. ΔpH shows the intersection of the connecting points with the horizontal axis at the point zero indicating pH_{pzc}, which was recorded as 4.5, as shown in Figure 7.

3.6.2. Study of pH. The pH of the solution is an important parameter controlling the adsorption process. The pH of

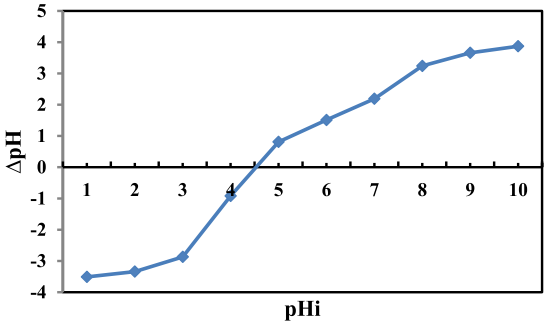

Figure 7. Points of zero charge for the carbon adsorbent.

solution greatly influences the adsorbent's surface, as a result, affects the adsorption and precipitation of metal ions in solution. The consequences of pH on elimination of selected metal ions by IONPs and acid-activated carbon were studied by increasing the pH from 2 to 8 at the starting adsorbate concentration (30 mg/L), the adsorbent dose (0.01 g) for 120 min at room a temperature of 25 °C. These various pH values resulted in a variation of arsenic, lead, and cadmium ion removal, which are exposed in Figure 8A,B. The outcomes

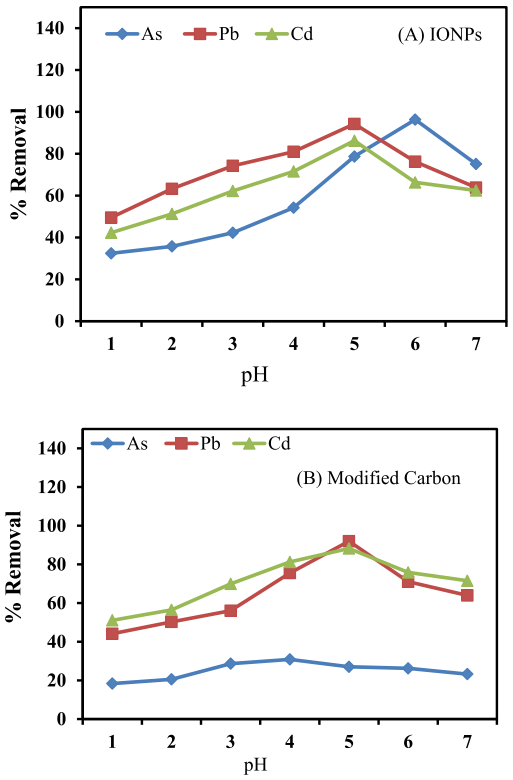

Figure 8. Effect of pH on (A) IONPs and (B) modified carbon, for the removal of As, Pb, and Cd ions.

show that removal of selected metal ions increases with the increase in pH. IONPs a showed maximum removal of arsenic 96.32% at pH 7, lead and cadmium 94.2 and 86.23%, respectively, at pH 6 while the modified carbon showed percentage removals of arsenic of 30.85% and lead of 91.96% at pH 5, whereas, the optimum pH 6 was recorded for cadmium with a removal percentage of 88.25%. A high positive charged density inhibited the accumulations of As, Pb, and Cd ions on the adsorbent binding site at low pH. By increasing pH, deprotonation effects increases negative charge density on the adsorbent promoting the interaction of adsorbate and adsorbent.[35] At a higher pH than optimum, the percentage removal of the selected metals decreases as a result of metal hydroxide formation. These metal hydroxide precipitates in the solution enabling additional adsorption study insignificant.[36] Similarly, the adsorption of metal ions on the adsorbent is also affected by the $pH_{pzc.}$ The point of zero charge is the pH at which the surface of adsorbents is neutral, containing an equal amount of positive and negative charges on the surface. Below this point, the surface is positively charged and beyond this point, it is negatively charged. It is easier to adsorb a cation on a negatively charged surface. However, some other interactions may also be stronger than electrostatic forces.[37] It is clear from

https://doi.org/10.1021/acsomega.3c05299
ACS Omega 2024, 9, 317−329

the results that optimum pH on, which high adsorption, was recorded was beyond the pH_{pzc} i.e. 4.5.

3.6.3. Study of Adsorbent Dose. The adsorbent dose is an important parameter because it determines the adsorption capacity of an adsorbent for a given initial concentration of the adsorbate. The adsorbent to adsorbate ratio significantly controls the overall adsorption process and optimization of adsorption is usually done with regard to the adsorbent dose in a fixed volume of adsorbate solution.[38] Effect of adsorbent dose on the selected metal ion adsorption was conducted by varying the dose from 0.01 to 0.06 g/50 mL of the adsorbent with a constant metal ion concentration for 120 min at room temperature. The percentage removal of metal ions becomes significant with the rise of the adsorbent dose. An adsorbent dose of 0.01 g of iron oxide showed 96.46% As, 85.33% Pb, and 81.3% Cd removal while the same dose of modified carbon showed removal of 30.86% As, 81.3% Pb, and 75.5% for As, Pb, and Cd ions, respectively. At a dose of 0.01 g, high adsorption capacity was noted for IONPs, i.e., As 144.7, Pb 128, and Cd 121.95 mg/g. The modified carbon showed adsorption capacity against As, Pb, and Cd were 46.3, 121.95, and 113.25 mg/g, respectively. With an increase of dose, a decrease in adsorption capacity of the adsorbent was observed, as shown in Figure 9A,B. By increasing the adsorbent dosage from 0.01 to 0.06 g/50 mL gives a rapid adsorption of arsenic, lead, and cadmium while further increase of adsorbent dose does not lead to a significant adsorption. The high percentage adsorption of lead and cadmium with a high adsorbent dose may be owed to accessibility of more dynamic sites on the adsorbent surface. Percentage adsorption of selected adsorbate decreased with further increase of adsorbent dose owing to the adsorbent particle aggregation, decreasing the surface area and active sites on adsorbents for metal ion adsorption. Percentage adsorption increases with increase of adsorbent dose while adsorption capacity decreases with increase of adsorbent dose.[39,40]

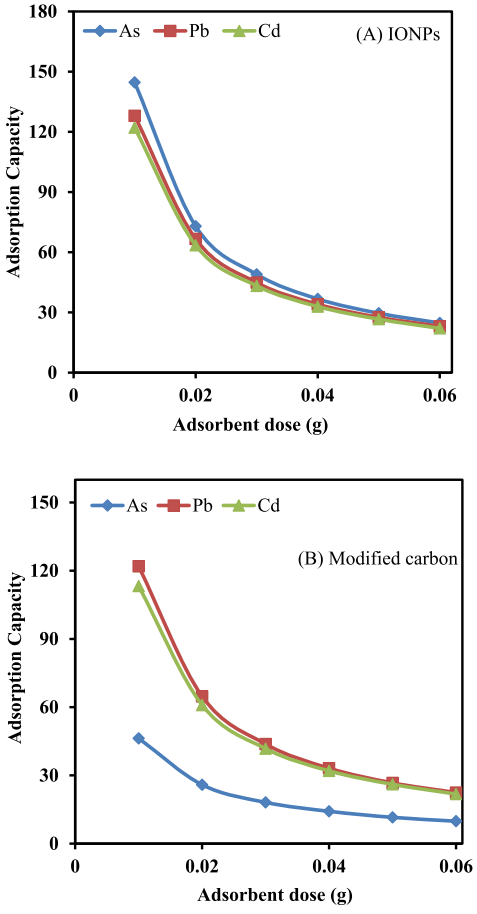

Figure 9. Effect of adsorbent dose on (A) IONPs and (B) modified carbon, for removal of As, Pb, and Cd ions.

3.6.4. Study of Adsorbate Initial Concentration. The significance of adsorbate initial concentration on the adsorption efficiency of synthesized IONPs and modified carbon was investigated at different initial concentrations of adsorbate, i.e., 10, 20, 30, 40, and 50 mg/L using a 0.01 g/50 mL adsorbent dose at pH-5 and pH-6. Figure 10A,B shows

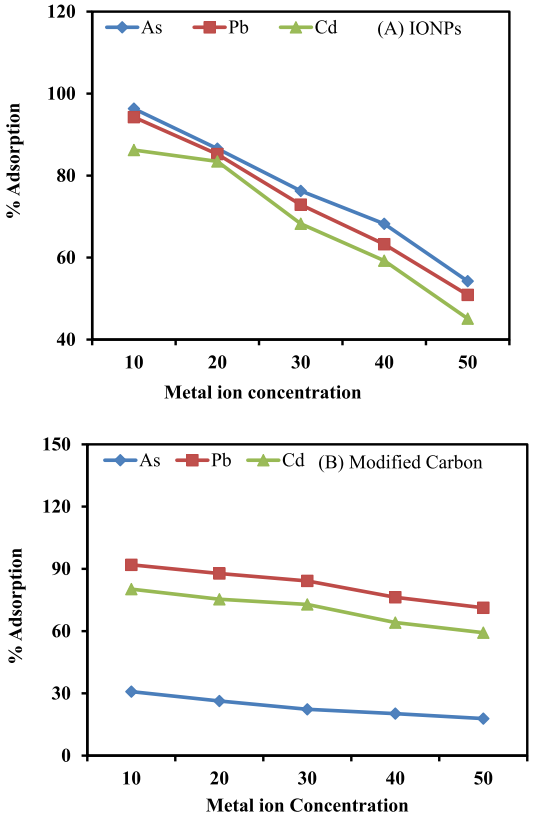

Figure 10. Effect of initial metal-ion concentration on (A) IONPs and (B) modified carbon, for the removal of As, Pb, and Cd ions.

that the percentage of arsenic, lead, and cadmium removal decreased by the increasing initial concentration of metal ions. The graphs reveal that percentage adsorption of under investigated metal ions were greater at the starting concentration (10 mg/L) of adsorbate. At a high concentration of feed solution, the active sites were rapidly filled leaving most of the metal ions in water. The surface area and the accessible active sites of adsorbent were relatively high at low concentration due to which the selected metal ions were easily adsorbed. On the other hand, the available active sites of adsorbent were less than the amount of adsorbate ions when the initial concentration of arsenic lead and cadmium was greater, and as a result, decreased the percentage removal of the selected metals.[41]

3.6.5. Effect of Contact Time. A study of time interval on adsorption of the selected adsorbate by IONPs and the

https://doi.org/10.1021/acsomega.3c05299
ACS Omega 2024, 9, 317−329

optimized carbon adsorbent was conducted with time variations of (5, 10, 15, 30, 60, 90, and 120 min) with an adsorbate initial concentration of 10 mg/L in 50 mL water. The results are depicted by Figure 11A,B. An adsorbent dose

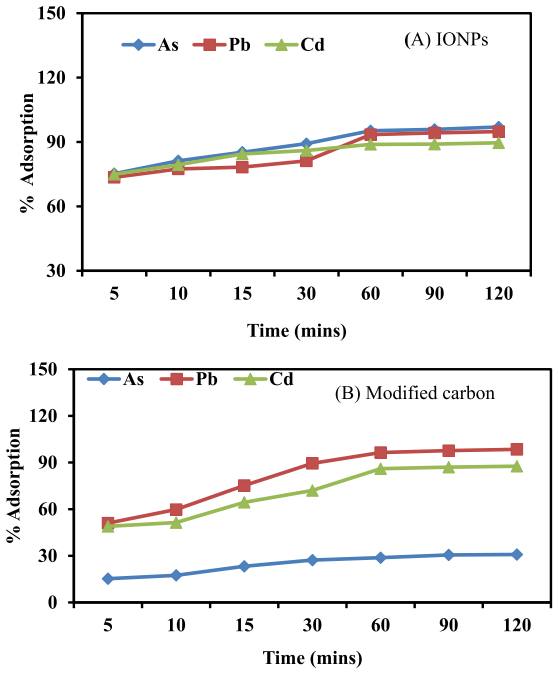

Figure 11. Effect of time on (A) IONPs and (B) modified carbon for removal of As, Pb, and Cd ions.

of 0.01 g was used at pH 5 for Cd and pH 6 for lead. An adsorption equilibrium was established within 60−90 min. Optimum contact time of arsenic lead and cadmium was 60 min with removal rates of 95.23, 93.45, and 89.9% by IONPs, respectively, while for modified activated carbon, the optimum contact time was noted to be 90 min with a percentage removal of 30.56% As, 97.65% Pb, and 87.01% Cd and no significant change in adsorption was observed after 60 min for IONPs and 90 min for the modified carbon adsorbent.[42]

3.6.6. Study of Temperature. A study of temperature variation on the removal of under investigated metal ions by the prepared adsorbents is publicized in Figure 12A,B. The graphs show that the percentage removal of metal ions increases with the rise in temperature in the range of 298−318 K, by keeping other parameters constant like optimum pH, adsorbent dose (0.01 g), and metal ion concentration (30 mg/L) for 60 min (for IONPs) and 90 min (for the carbon adsorbent). It signifies that adsorption is more significant at a relatively high temperature of 318 K. The high temperature may create new active sites on the adsorbent surface. But above 318 K, percentage adsorption decreased due to desorption of metal ions. Generally, chemical adsorption is preferential by a high temperature while low temperature favors physical adsorption.[43]

3.7. Adsorption Isotherm Models. An adsorption isotherm study was conducted to recognize the correlation between the adsorbed metal ions and prepared adsorbents by keeping the temperature constant. Experimental adsorption data were evaluated by applying adsorption isotherm Freundlich and Langmuir models to ascertain adsorption capacity of adsorbents at the equilibrium against the selected adsorbate in solution. The Freundlich isotherm model in linear form is represented by VI

$$\mathrm{Log}q_e = \mathrm{Log}\ K_f + 1/n\ \mathrm{Log}\ C_e \quad \text{(VI)}$$

where; q_e—amount of adsorbate adsorbed (mg/g), K_f—Freundlich constant equal to the intercept, and $1/n$—slope of the plot (C_e vs q_e).

The Langmuir isotherm model is represented by the equation below

$$1/q_e = 1/K_L\ q_{max} \cdot 1/C_e + 1/q_{max} \quad \text{(VII)}$$

where; q_{max}—highest adsorption capacity and K_L—Langmuir constant.

The below equation was evaluated for separation factor (R_L) showing the adsorption possibility

$$R_L = 1/1 + C_o \times K_L \quad \text{(VIII)}$$

The relevant isotherms model parameters q_{max}, K_L, R_L, and R^2 for the Langmuir isotherm and K_f, $1/n$ and R^2 for the Freundlich isotherm are tabulated in Table 1. It is obvious from the table that both models have the close values of R^2 to 0.99 indicating the usefulness of both models but still Langmuir's isotherm was the best fitted on experimental data with a greater linear correlation coefficient R^2 value than that of the Freundlich isotherm for almost all processes. It verifies the monolayer adsorption of the selected metal ions on adsorbents. The value of $R_L < 1$ for both IONPs and modified carbon which favors the adsorption. The calculated maximum adsorption capacities by the Langmuir model for most of the selected metal ions were in close resemblance with the experimental data.

3.8. Temkin Isotherm. The Temkin isotherm presupposes a linear decline in sorption heat and a homogeneous distribution of binding energies (up to a maximum binding

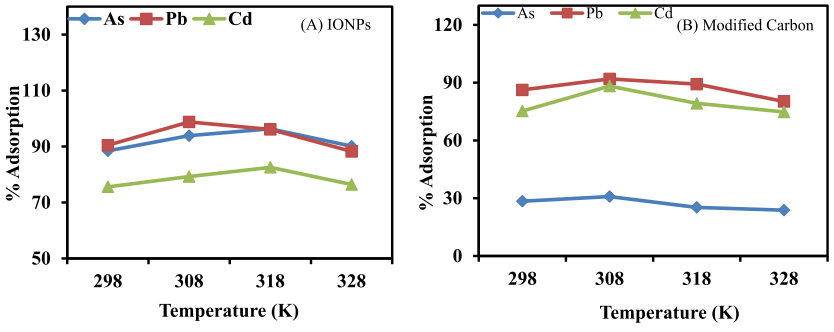

Figure 12. Effect of temperature on (A) IONPs and (B) modified carbon, for removal of As, Pb, and Cd ions.

https://doi.org/10.1021/acsomega.3c05299
ACS Omega 2024, 9, 317−329

Table 1. Types of Isotherms with Different Parameters

		IONPS			modified carbon		
type of isotherm	parameters	As	Pb	Cd	As	Pb	Cd
Langmuir	q_{max} (mg/g)	142.85	125	142.86	71.428	166.666	142.857
	K_L (L/mg)	1.75	1.142	0.333	0.039	0.461	0.175
	R_L	0.018	0.028	0.09	0.456	0.067	0.16
	R^2	0.961	0.983	0.973	0.999	0.995	0.997
Freundlich	K_f	6.122	0.272	5.306	2.006	5.675	4.345
	$1/n$	0.266	0.272	0.313	0.601	0.469	0.561
	R^2	0.977	0.965	0.84	0.992	0.978	0.97
Temkin	K_T (J/mol)	1.89	1.74	1.54	1.12	2.64	1.12
	B_T (J/mol)	108.57	111.16	104.15	150.41	54	53.17
	R^2	0.974	0.986	0.898	0.993	0.993	0.991
Dobinin−Radushkevich	q_{max} (mg/g)	118.6	113.74	111.05	39.76	144.17	125.96
	E (kJ/mol)	2.36	2.24	1.00	0.24	1.29	0.71
	R^2	0.875	0.894	0.981	0.908	0.88	0.898

energy). This model predicts that, as a result of indirect adsorbate/adsorbent interactions, the heat of adsorption of all molecules in the layer would decrease linearly with coverage.[44,45] Generally, the Temkin isotherm has been used as follows

$$q_e = B \ln K_T + B_T \ln C_e \quad \text{(IX)}$$

By linear plotting of q_e vs ln C_e, the Temkin model constants K_T and $B = RT/b$ can be calculated, which provide information about the heat of adsorption (J/mol). The positive values of B_T, as tabulated in Table 1, show that the adsorption process is exothermic in the concentration study.

3.9. Dubinin−Radushkevich Isotherm. The Dubinin−Radushkevich model, which quantifies the adsorption energy in terms of the adsorption potential (ε), is the final isotherm. This model is used to determine the type of adsorption, physical or chemical, based on the value of apparent adsorption energy (E).If $E < 8$ kJ/mol, it indicates that the adsorption is physical; $8 < E < 16$ kJ/mol indicates that the adsorption is a chemical ion exchange; and when $E > 16$, it shows chemical adsorption. The following equations can explain the Dubinin−Radushkevich isotherm model.[46,47]

$$\ln q_e = \ln q_m - \beta\varepsilon^2 \quad \text{(X)}$$

$$\varepsilon = RT \ln(1 + 1/C_e) \quad \text{(XI)}$$

$$E = 1/\sqrt{2\beta} \quad \text{(XII)}$$

where β is the mean free energy constant of adsorption, q_m is monolayer coverage, ε is the Polanyi potential (kJ/Mol), R is universal gas constant, T is the absolute temperature, and E is mean adsorption energy. The range of mean free energy (0.24−2.36 kJ/mol) (Table 1) using this model indicates the physisorption nature of all the adsorption processes in the concentration range.

3.10. Kinetic Models Study. The adsorption mechanism and rate of adsorption of selected adsorbate on IONPs and modified carbon adsorbent were probed by pseudo-first-order (PFO) and pseudo-second-order (PSO) kinetic models.

The linear form of the pseudo first order kinetic equation is given by

$$\ln(q_e - q_t) = \ln q_e - K_1 t \quad \text{(XIII)}$$

where; q_t—amount of adsorbate adsorbed at time t. K_1—adsorption rate constant for the first order.

The linear form of pseudo-second order is given by

$$t/q_t = 1/K_2 q_e^2 + t/q_e \quad \text{(XIV)}$$

where K_2 is the rate constant for the second order.

The rate constants K_1, K_2, and R^2 values were calculated from the plotting of ln $(q_e - q_t)$ vs t for PFO and t/q_t vs t for PSO kinetic models, as plotted in Figure 13A,B. The resulting kinetic parameters are listed in Table 2. The table shows low correlation coefficient R^2 values for PFO and high differences were observed in adsorption capacity of experimental (q_e exp)

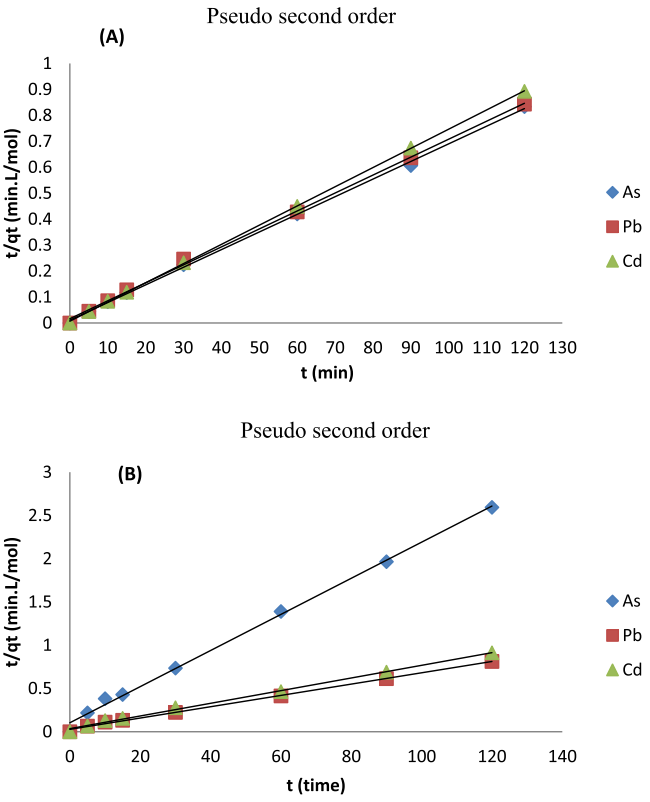

Figure 13. (A) PSO kinetics for adsorption of metal ions on IONP and (B) PSO kinetic plot for adsorption of metal ions on modified carbon.

https://doi.org/10.1021/acsomega.3c05299
ACS Omega 2024, 9, 317−329

Table 2. Types of Kinetic Models with Different Parameters

	parameters	IONPS			modified carbon		
order of reaction	q_e exp(mg.g)	As	Pb	Cd	As	Pb	Cd
PFO	q_e cal(mg/g)	40.85	53.46	4.237	22.131	76.401	78.64
	K_1 (min^{-1})	−0.001	−0.001	−0.0004	−0.0004	−0.0006	−0.0006
	R^2	0.984	0.901	0.893	0.957	0.96	0.945
PSO	q_e cal(mg/g)	166.67	166.67	142.85	50	166.67	142.85
	K_2 (g mg^{-1} min^{-1})	0.0036	0.0023	0.0082	0.00389	0.0014	0.0014
	R^2	0.999	0.998	0.999	0.997	0.997	0.996
intraparticle diffusion	K_{diff}	3.4	3.98	2.22	2.6	7.93	7.12
	C	111.5	102.6	113.3	21.15	73.07	62.88
	R^2	0.875	0.936	0.784	0.843	0.819	0.897

and calculated values of adsorption capacities (q_e cal) by the PSO model and do not fit to the adsorption data. Therefore, adsorption of adsorbate was described by PSO kinetic model. The PSO model was found to fit on experimental data well with a high correlation coefficient (R^2) value of 0.99 for all the selected metal-ion adsorption and also have a close resemblance between experimental and calculated adsorption capacities. The PSO model was also followed by adsorption of As, Pb, and Cd ions on different adsorbents as reported in literature studies.[48,49]

Another model called the Weber and Morris model (an intraparticle diffusion model) was used to test whether intraparticle diffusion (IPD) or boundary layer diffusion controls Pb(II) adsorption on R. B. seeds and AC. According to this model, IPD is the rate-limiting step, if a plot of the amount of an adsorbate that is adsorbed against the square root of the contact duration results in a straight line that passes through the origin.[50,51] The equation for this model is given by

$$Q_t = K_{diff} t^{1/2} + I \quad \text{(XV)}$$

where Q_t is amount of adsorbate at a specific time, K_{diff} is the IPD rate constant (mg g^{-1} $min^{-0.5}$), and I is the intercept. The plotting of $t^{1/2}$ vs Q_t, as shown in Figure 14A,B, shows that adsorption took place in two steps. In the first step, the adsorption was rapid, which may be correlated to the external surface or boundary layer diffusion while in the second step, no apparent change was observed. The extrapolation of the data does not pass through the origin, and also the R^2 values (shown in Table 1) are not close to 1. Hence, it is not well fitted to the Morris model and adsorption is more likely boundary layer controlled.

3.11. Influence of Coexisting Ions. The presence of other metals and HM ions may interfere with the adsorptive removal of one HM ion in wastewater. It is crucial to understand the adsorption of HMs in multicomponent systems in order to properly explore the effectiveness and practical applications of the adsorbents. The true interactive behavior of the HMs in the multicomponent sorption system may be seen through competitive adsorption and three main types of impacts are possible: synergism, antagonism, and noninteraction.[44]

The ratio of the maximum uptake capacity for one HM ion in the multicomponent system (q_{mix}) to the uptake capacity for the same HM ions present in the single system (q_o) determines the impact of the ionic interactions on the multicomponent sorption system.

Mathematically, the interaction factor (R_{q_e}) is expressed in the equation

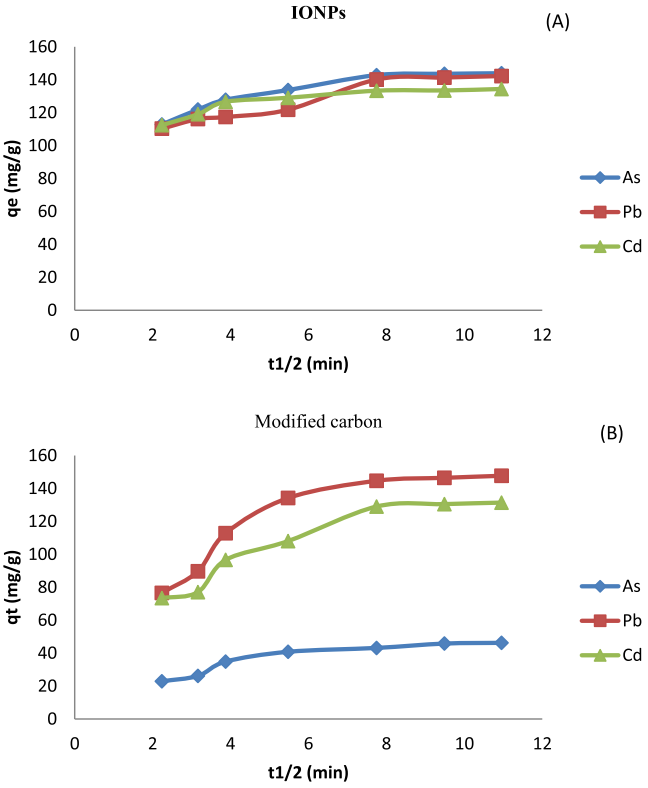

Figure 14. (A) IPD model for adsorption of metal ions on IONPs and (B) IPD model for adsorption of metal ions on modified carbon.

$$R_{q_e} = \frac{q_{mix}}{q_o} \quad \text{(XVI)}$$

where q_{mix} is the adsorption capacity of any metal in the multicomponent solution and q_e is the adsorption capacity of the same metal in a single component solution under the same operating conditions. R_{q_e} compares the adsorbent efficiency in a single phase system to that of the multiphase system. If $\frac{q_{mix}}{q_o} > 1$, it suggests a synergism effect, and if $\frac{q_{mix}}{q_o} = 1$, indicating noninteraction. If $\frac{q_{mix}}{q_o} < 1$, it suggests to the antagonism effect.[52] The adsorption capacity of adsorbents against the target ions in a single component system and in a multi component system has been shown in Figure 15A,B. The optimum conditions for this study were pH = 6, adsorbent dose of 0.01 g, and initial metal concentration of 10 mg/g in 50 mL of water at 298 K. The data show that adsorption capacity

https://doi.org/10.1021/acsomega.3c05299
ACS Omega 2024, 9, 317−329

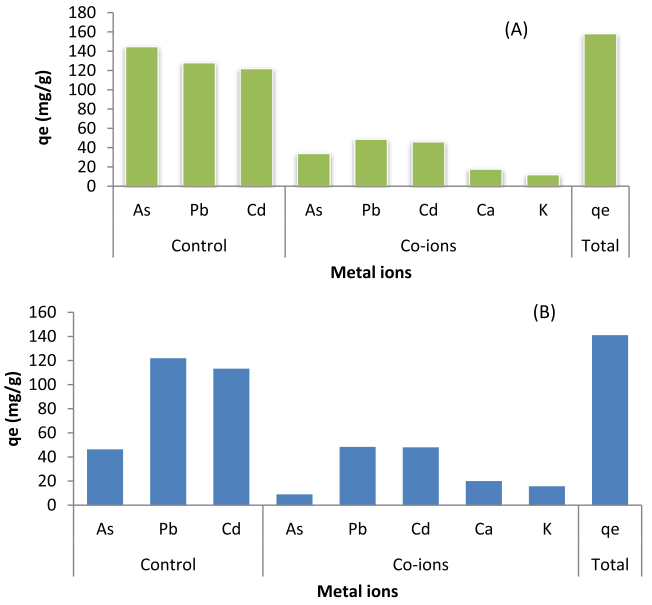

Figure 15. (A) Adsorption capacity of IONPS in multicomponent solution and (B) adsorption capacity of modified carbon in multicomponent solution.

of IONPS for As decreases from 144.7 to 33.9 mg/g, Pb from 128 to 48.75 mg/g, and Cd from 121.95 to 48.75 mg/g against the selected metal ions decreased in the multiphase system. Similarly, the adsorption capacity of modified carbon against As decreased from 46.3 to 8.95 mg/g, Pb from 121.95 to 48.4 mg/g, and Cd from 113.25 to 47.95 mg/g. The adsorption rate of alkali metal K^+ and alkaline earth metal ions Ca^+ was poor compared to the selected HM ions. The competition for available active sites between the targeted metal ions and other alkali and alkaline metals generated in the solution can be the reason for the observed result. A similar result was reported by Huang et al. using modified bagasse for metal-ion adsorption in binary and multicomponent systems.[53]

3.12. Reusability of Adsorbent. Reusability of an adsorbent is a significant and economically enviable stair for wide use of the adsorbent. Reusability of the adsorbent decreases the operational expenditure. The desorption ability of the adsorbent was examined in such studies, and the detached metal ions may be reused in the key associated processes. The spent adsorbents were regenerated using hydrochloric acid as a desorbing medium and then utilized back in a new batch study to test the elimination of the selected metal ions. Hydrochloric acid (HCl) is mostly used for the desorption reagent in the acid regeneration method as it has no oxidation property, and chloride ion has a slight effect on adsorption of most HMs.[54] The obtained As, Pb, and Cd ion removal efficiencies of IONPs and modified carbon adsorbent for five recycling runs are plotted in Figure 16A,B. Regeneration success of HCl is attributed to the substitution of metal ions by H^+ ions (protonation) on the surface of adsorbent. It was seen that in regeneration cycles of IONPs, arsenic-ion removal efficiency gradually decreased from 144.8 to 45.67 mg/g, lead from 128.15 to 41.65 mg/g, and cadmium from 122.10 to 31.20 mg/g. Similarly, in regeneration cycles of modified carbon, arsenic adsorption capacity decreased from 46.4 to 19.4 mg/g, lead from 122.05 to 54.24 mg/g, and cadmium from 111.35 to 52.12 mg/g.

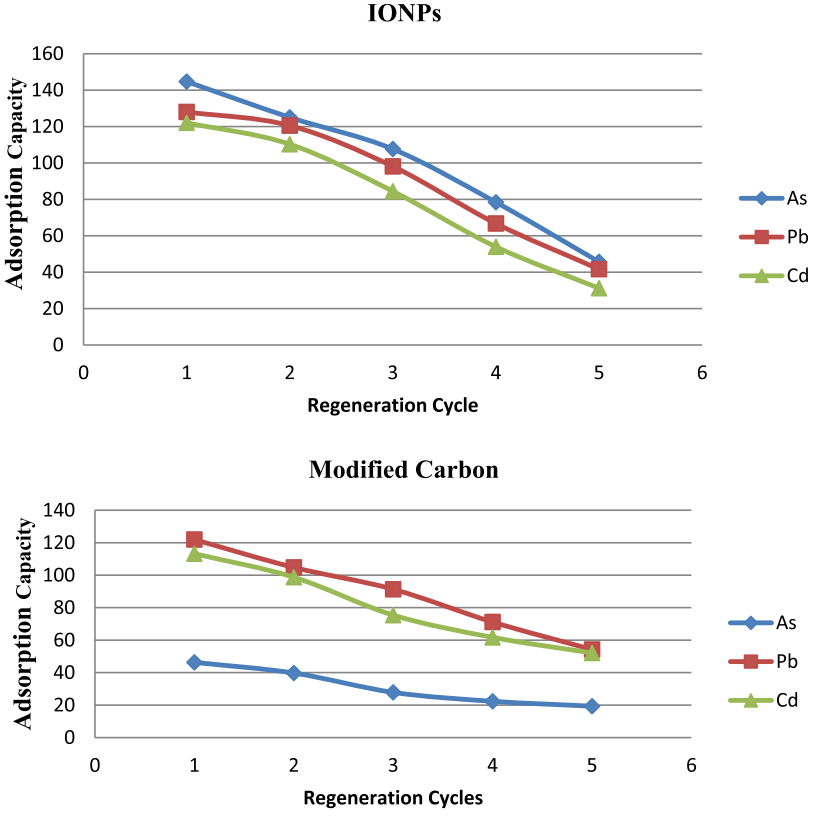

Figure 16. (A) Adsorption capacities (q_e) of regenerated IONPs for five cycles and (B) adsorption capacities (q_e) of regenerated carbon adsorbent for five cycles.

https://doi.org/10.1021/acsomega.3c05299
ACS Omega 2024, 9, 317−329

4. CONCLUSIONS

In the current study, the plant *Capparis deciduas* extract played a prominent role in reduction and stabilization of IONPs and *P. hysterophorus* plants was used as cost-effective, nontoxic, and eco-friendly carbon adsorbent preparation on a large scale. The main concern about the nanoparticles is their stability, which was stabilized by the capping agents present in plants. The synthesized IONPs and carbon adsorbent were pictured out by means of various systems like UV−vis, FT-IR, SEM, EDX, and XRD. The factors that affect the adsorbate and adsorbent interactions like pH, adsorbate initial concentration, time interval, and adsorbent dose were considered, and each parameter was optimized. The synthesized IONPs at optimum conditions showed 144.7,128.01, and 122.1 mg/g adsorption capacity against As, Pb, and Cd, respectively. While the activated carbon under optimum conditions showed 46.35,, 121.95, and 113.25 mg/g adsorption capacity against As, Pb, and Cd, respectively. The influence of Ca^{+} and K^{+} adsorption was poor in the multicomponent system. The q_e of IONPs and the carbon adsorbent gradually decreased in the adsorption process of As, Pb, and Cd ions in five consecutive cycles. Thus, the synthesized IONPs and acid-activated carbon adsorbent were successfully used to remove selected metal ions from wastewater.

■ ASSOCIATED CONTENT

Data Availability Statement

All the data generated and analyzed has already been incorporated into the study.

■ AUTHOR INFORMATION

Corresponding Author

Ijaz Ahmad − *Department of Chemistry, Kohat University of Science & Technology, Kohat 26000, Pakistan;* orcid.org/0000-0002-9139-1611; Email: drijaz_chem@yahoo.com

Authors

Ali Rehman − *Department of Chemistry, Kohat University of Science & Technology, Kohat 26000, Pakistan*

Abdul Naeem − *National Center of Excellence in Physical Chemistry, University of Peshawar, Peshawar 25120, Pakistan*

Fozia Fozia − *Biochemistry Department, Khyber Medical University Institute of Dental Sciences, Kohat 26000, Pakistan;* orcid.org/0000-0002-4554-7427

Mikhlid H. Almutairi − *Zoology Department, College of Science, King Saud University, Riyadh 11451, Saudi Arabia;* orcid.org/0000-0002-0337-6412

Madeeha Aslam − *Department of Chemistry, Kohat University of Science & Technology, Kohat 26000, Pakistan*

Muhammad Israr − *Department of Chemistry, Kohat University of Science & Technology, Kohat 26000, Pakistan*

Bader O. Almutairi − *Zoology Department, College of Science, King Saud University, Riyadh 11451, Saudi Arabia*

Zia Ullah − *College of Professional Studies, Northeastern University, Boston, Massachusetts 02115, United States*

Complete contact information is available at: https://pubs.acs.org/10.1021/acsomega.3c05299

Author Contributions

Conceptualization, IA and AN; data curation, IA; formal analysis, AR, IA, and AN; funding acquisition, MH.A and BO.A; investigation, AR; methodology, AR; project administration, IA; resources, IA, AN, and FF; supervision: IA and AN; visualization, MA, MI, and MH.A; writing−original draft, AR, MA, and MI; and writing−review and editing, IA, AN, FF, MH.A, BO.A, and ZU.

Notes

The authors declare no competing financial interest.

■ ACKNOWLEDGMENTS

The authors extend their appreciation to the Researchers Supporting Project number (RSP2023R191), King Saud University, Riyadh, Saudi Arabia.

■ REFERENCES

(1) Pérez, H.; Quintero García, O. J.; Amezcua-Allieri, M. A.; Rodríguez Vázquez, R. "Nanotechnology as an efficient and effective alternative for wastewater treatment: an overview,". *Water Sci. Technol.* **2023**, *87*, 2971−3001.

(2) Naseem, T.; Durrani, T. "The role of some important metal oxide nanoparticles for wastewater and antibacterial applications: A review,". *Environ. Chem. Ecotoxicol.* **2021**, *3*, 59−75.

(3) Ijaz, I.; Gilani, E.; Nazir, A.; Bukhari, A. "Detail review on chemical, physical and green synthesis, classification, characterizations and applications of nanoparticles,". *Green Chem. Lett. Rev.* **2020**, *13*, 223−245.

(4) Tadic, M.; Trpkov, D.; Kopanja, L.; Vojnovic, S.; Panjan, M. Hydrothermal synthesis of hematite (α-Fe2O3) nanoparticle forms: Synthesis conditions, structure, particle shape analysis, cytotoxicity and magnetic properties. *J. Alloys Compd.* **2019**, *792*, 599−609.

(5) Li, Y.; Huang, Y.; Zheng, Y.; Huang, R.; Yao, J. Facile and efficient synthesis of α-Fe2O3 nanocrystals by glucose-assisted thermal decomposition method and its application in lithium ion batteries. *J. Power Sources* **2019**, *416*, 62−71.

(6) Besenhard, M. O.; LaGrow, A. P.; Hodzic, A.; Kriechbaum, M.; Panariello, L.; Bais, G.; Loizou, K.; Damilos, S.; Margarida Cruz, M.; Thanh, N. T. K.; et al. "Co-precipitation synthesis of stable iron oxide nanoparticles with NaOH: New insights and continuous production via flow chemistry,". *Chem. Eng. J.* **2020**, *399*, 125740.

(7) Bokov, D.; Turki Jalil, A.; Chupradit, S.; Suksatan, W.; Javed Ansari, M.; Shewael, I. H.; Valiev, G. H.; Kianfar, E. "Nanomaterial by sol-gel method: synthesis and application,". *Adv. Mater. Sci. Eng.* **2021**, *2021*, 1−21.

(8) Escorcia, N. J.; LiBretto, N. J.; Miller, J. T.; Li, C. W. "Colloidal synthesis of well-defined bimetallic nanoparticles for nonoxidative alkane dehydrogenation,". *ACS Catal.* **2020**, *10*, 9813−9823.

(9) Nair, G. M.; Sajini, T.; Mathew, B. "Advanced green approaches for metal and metal oxide nanoparticles synthesis and their environmental applications,". *Talanta Open* **2022**, *5*, 100080.

(10) Yadanaparthi, S. K. R.; Graybill, D.; von Wandruszka, R. "Adsorbents for the removal of arsenic, cadmium, and lead from contaminated waters,". *J. Hazard Mater.* **2009**, *171*, 1−15.

(11) Arita, A.; Costa, M. "Epigenetics in metal carcinogenesis: nickel, arsenic, chromium and cadmium,". *Metallomics* **2009**, *1*, 222−228.

(12) Abdel-Halim, S.; Shehata, A.; El-Shahat, M. "Removal of lead ions from industrial waste water by different types of natural materials,". *Water Res.* **2003**, *37*, 1678−1683.

(13) Xing, W.; Liang, J.; Tang, W.; He, D.; Yan, M.; Wang, X.; Luo, Y.; Tang, N.; Huang, M. "Versatile applications of capacitive deionization (CDI)-based technologies,". *Desalination* **2020**, *482*, 114390.

(14) Chen, A. S.; Wang, L.; Sorg, T. J.; Lytle, D. A. "Removing arsenic and co-occurring contaminants from drinking water by full-scale ion exchange and point-of-use/point-of-entry reverse osmosis systems,". *Water Res.* **2020**, *172*, 115455.

(15) Minhas, M. B.; Jande, Y.; Kim, W.-S. "Combined reverse osmosis and constant-current operated capacitive deionization system for seawater desalination,". *Desalination* **2014**, *344*, 299−305.
(16) Bezzina, J. P.; Ruder, L. R.; Dawson, R.; Ogden, M. D. "Ion exchange removal of Cu (II), Fe (II), Pb (II) and Zn (II) from acid extracted sewage sludge-Resin screening in weak acid media,". *Water Res.* **2019**, *158*, 257−267.
(17) Qasem, N. A.; Mohammed, R. H.; Lawal, D. U. "Removal of heavy metal ions from wastewater: A comprehensive and critical review,". *npj Clean Water* **2021**, *4*, 36.
(18) Mariana, M.; Hps, A. K.; Mistar, E.; Yahya, E. B.; Alfatah, T.; Danish, M.; Amayreh, M. "Recent advances in activated carbon modification techniques for enhanced heavy metal adsorption,". *J. Water Proc. Eng.* **2021**, *43*, 102221.
(19) Kaur, M.; Kumari, S.; Sharma, P. "Removal of Pb (II) from aqueous solution using nanoadsorbent of Oryza sativa husk: Isotherm, kinetic and thermodynamic studies,". *Biotechnol. Rep.* **2020**, *25*, No. e00410.
(20) Al-Khaldi, F. A.; Al-Khaldi, F. A.; Abusharkh, B.; Khaled, M.; Atieh, M. A.; Nasser, M.; laoui, T.; Saleh, T. A.; Agarwal, S.; Tyagi, I.; et al. "Adsorptive removal of cadmium (II) ions from liquid phase using acid modified carbon-based adsorbents,". *J. Mol. Liq.* **2015**, *204*, 255−263.
(21) Calderón, C.; Levio-Raiman, M.; Diez, M. "Cadmium removal for marine food application: Comparative study of different adsorbents,". *Int. J. Environ. Sci. Technol.* **2022**, *19*, 8871−8884.
(22) Varshney, S.; Jain, P.; Srivastava, S. "Removal and recovery of chromium from e-waste by functionalized wood pulp: a green bio-hydrometallurgical approach,". *Natl. Acad. Sci. Lett.* **2019**, *42*, 99−103.
(23) Upadhyay, U.; Sreedhar, I.; Singh, S. A.; Patel, C. M.; Anitha, K. "Recent advances in heavy metal removal by chitosan based adsorbents,". *Carbohydr. Polym.* **2021**, *251*, 117000.
(24) Shrestha, B.; Shabbir, A.; Adkins, S. "Parthenium hysterophorus in N epal: a review of its weed status and possibilities for management,". *Weed Res.* **2015**, *55*, 132−144.
(25) Khalil, A. T.; Ovais, M.; Ullah, I.; Ali, M.; Shinwari, Z. K.; Maaza, M. "Biosynthesis of iron oxide (Fe2O3) nanoparticles via aqueous extracts of Sageretia thea (Osbeck.) and their pharmacognostic properties,". *Green Chem. Lett. Rev.* **2017**, *10*, 186−201.
(26) Chauhan, S.; Upadhyay, L. S. B. "Biosynthesis of iron oxide nanoparticles using plant derivatives of Lawsonia inermis (Henna) and its surface modification for biomedical application,". *Nanotechnol. Environ. Eng.* **2019**, *4*, 8−10.
(27) Wu, H.; Chen, R.; Du, H.; Zhang, J.; Shi, L.; Qin, Y.; Yue, L.; Wang, J. "Synthesis of activated carbon from peanut shell as dye adsorbents for wastewater treatment,". *Adsorpt. Sci. Technol.* **2019**, *37*, 34−48.
(28) Nazar, S.; Hussain, M. A.; Khan, A.; Muhammad, G.; Tahir, M. N. "Capparis decidua Edgew (Forssk.): A comprehensive review of its traditional uses, phytochemistry, pharmacology and nutrapharmaceutical potential,". *Arab. J. Chem.* **2020**, *13*, 1901−1916.
(29) Groiss, S.; Selvaraj, R.; Varadavenkatesan, T.; Vinayagam, R. "Structural characterization, antibacterial and catalytic effect of iron oxide nanoparticles synthesised using the leaf extract of Cynometra ramiflora,". *J. Mol. Struct.* **2017**, *1128*, 572−578.
(30) Caccamo, M. T.; Zammuto, V.; Spanò, A.; Gugliandolo, C.; Magazù, S. "Hydrating Capabilities of the Biopolymers Produced by the Marine Thermophilic Bacillus horneckiae SBP3 as Evaluated by ATR-FTIR Spectroscopy,". *Materials* **2022**, *15*, 5988.
(31) Moalla, S.; Ammar, I.; Fauconnier, M.-L.; Danthine, S.; Blecker, C.; Besbes, S.; Attia, H. "Development and characterization of chitosan films carrying Artemisia campestris antioxidants for potential use as active food packaging materials,". *Int. J. Biol. Macromol.* **2021**, *183*, 254−266.
(32) D'Souza, L.; Devi, P.; Divya Shridhar, M.; Naik, C. G. "Use of Fourier Transform Infrared (FTIR) spectroscopy to study cadmium-induced changes in Padina tetrastromatica (Hauck),". *Anal. Chem. Insights* **2008**, *3*, 117739010800300.
(33) Ricci, A.; Olejar, K. J.; Parpinello, G. P.; Kilmartin, P. A.; Versari, A. "Application of Fourier transform infrared (FTIR) spectroscopy in the characterization of tannins,". *Appl. Spectrosc. Rev.* **2015**, *50*, 407−442.
(34) Tiernan, H.; Byrne, B.; Kazarian, S. G. "ATR-FTIR spectroscopy and spectroscopic imaging for the analysis of biopharmaceuticals,". *Spectrochim. Acta, Part A* **2020**, *241*, 118636.
(35) Krishnamoorthy, R.; Govindan, B.; Banat, F.; Sagadevan, V.; Purushothaman, M.; Show, P. L. "Date pits activated carbon for divalent lead ions removal,". *J. Biosci. Bioeng.* **2019**, *128*, 88−97.
(36) Baby, R.; Hussein, M. Z. "Ecofriendly approach for treatment of heavy-metal-contaminated water using activated carbon of kernel shell of oil palm,". *Materials* **2020**, *13*, 2627.
(37) Dhahri, R.; Yılmaz, M.; Mechi, L.; Alsukaibi, A. K. D.; Alimi, F.; ben Salem, R.; Moussaoui, Y. "Optimization of the preparation of activated carbon from prickly pear seed cake for the removal of lead and cadmium ions from aqueous solution,". *Sustainability* **2022**, *14*, 3245.
(38) Azarpira, H.; Mahdavi, Y.; Balarak, D. "Removal of Cd (II) by adsorption on agricultural waste biomass,". *Der Pharma Chem.* **2016**, *8*, 61−67.
(39) Balarak, D.; Azarpira, H.; Mostafapour, F. K. Thermodynamics of removal of cadmium by adsorption on Barley husk biomass,". *Der Pharma Chem.* **2016**, *8*, 243−247.
(40) Fito, J.; Tibebu, S.; Nkambule, T. T. "Optimization of Cr (VI) removal from aqueous solution with activated carbon derived from Eichhornia crassipes under response surface methodology,". *BMC Chem.* **2023**, *17*, 4.
(41) Altunkaynak, Y.; Canpolat, M.; Yavuz, O.·. "Adsorption of cobalt (II) ions from aqueous solution using orange peel waste: equilibrium, kinetic and thermodynamic studies,". *J. Iran. Chem. Soc.* **2022**, *19*, 2437−2448.
(42) Awwad, A. M.; Amer, M. A. "Adsorption of Pb (II), Cd (II), and Cu (II) ions onto SiO2/kaolinite/Fe2O3 composites: modeling and thermodynamics properties,". *Chem. Int.* **2022**, *8*, 95−100.
(43) Jiang, C.; Wang, X.; Wang, G.; Hao, C.; Li, X.; Li, T. "Adsorption performance of a polysaccharide composite hydrogel based on crosslinked glucan/chitosan for heavy metal ions,". *Composites, Part B* **2019**, *169*, 45−54.
(44) Mahvi, A. H.; Balarak, D.; Bazrafshan, E. "Remarkable reusability of magnetic Fe3O4-graphene oxide composite: a highly effective adsorbent for Cr (VI) ions,". *Int. J. Environ. Anal. Chem.* **2023**, *103*, 3501−3521.
(45) Bazrafshan, E.; Sobhanikia, M.; Mostafapour, F.; Kamani, H.; Balarak, D. "Chromium biosorption from aqueous environments by mucilaginous seeds of Cydonia oblonga: kinetic and thermodynamic studies,". *Global NEST J.* **2017**, *19*, 269−277.
(46) Ullah, R.; Sun, J.; Gul, A.; Bai, S. "One-step hydrothermal synthesis of TiO2-supported clinoptilolite: An integrated photocatalytic adsorbent for removal of crystal violet dye from aqueous media,". *J. Environ. Chem. Eng.* **2020**, *8*, 103852.
(47) Kord Mostafapour, F.; Mahvi, A. H.; Khatibi, A. D.; Khodadadi Saloot, M.; Mohammadzadeh, N.; Balarak, D. "Adsorption of lead (II) using bioadsorbent prepared from immobilized Gracilaria corticata algae: thermodynamics, kinetics and isotherm analysis,". *Desalination Water Treat.* **2022**, *265*, 103−113.
(48) Bilal, M.; Ali, J.; Hussain, N.; Umar, M.; Shujah, S.; Ahmad, D. "Removal of Pb (II) from wastewater using activated carbon prepared from the seeds of Reptonia buxifolia,". *J. Serb. Chem. Soc.* **2020**, *85*, 265−277.
(49) Kavand, M.; Eslami, P.; Razeh, L. "The adsorption of cadmium and lead ions from the synthesis wastewater with the activated carbon: Optimization of the single and binary systems,". *J. Water Proc. Eng.* **2020**, *34*, 101151.
(50) Al-Musawi, T. J.; Mengelizadeh, N.; Al Rawi, O.; Balarak, D. "Capacity and modeling of acid blue 113 dye adsorption onto chitosan magnetized by Fe2O3 nanoparticles,". *J. Polym. Environ.* **2022**, *30*, 344−359.

https://doi.org/10.1021/acsomega.3c05299
ACS Omega 2024, 9, 317−329

(51) Sillanpää, M.; Mahvi, A. H.; Balarak, D.; Khatibi, A. D. ″Adsorption of Acid orange 7 dyes from aqueous solution using Polypyrrole/nanosilica composite: Experimental and modelling,″. *Int. J. Environ. Anal. Chem.* **2023**, *103*, 212−229.
(52) Bayuo, J.; Rwiza, M. J.; Sillanpää, M.; Mtei, K. M. ″Removal of heavy metals from binary and multicomponent adsorption systems using various adsorbents-a systematic review,″. *RSC Adv.* **2023**, *13*, 13052−13093.
(53) Huang, S.; Jin, S.; Wang, Y.; Liu, J.; Yu, J.; Liu, D.; Chi, R. ″Selective adsorption of heavy metal ions from aqueous solution by modified bagasse,″. *Chem. Ecol.* **2020**, *36*, 839−854.
(54) Duan, C.; Ma, T.; Wang, J.; Zhou, Y. ″Removal of heavy metals from aqueous solution using carbon-based adsorbents: A review,″. *J. Water Proc. Eng.* **2020**, *37*, 101339.

https://doi.org/10.1021/acsomega.3c05299
ACS Omega 2024, 9, 317−329